Interplay of F−H(...)F Hydrogen Bonds and P(...)N Pnicogen Bonds.

ARTICLE *in* THE JOURNAL OF PHYSICAL CHEMISTRY A · AUGUST 2012

Impact Factor: 2.69 · DOI: 10.1021/jp307083g · Source: PubMed

THE JOURNAL OF PHYSICAL CHEMISTRY A

Article

pubs.acs.org/JPCA

Interplay of F−H···F Hydrogen Bonds and P···N Pnicogen Bonds

Janet E. Del Bene*

Department of Chemistry, Youngstown State University, Youngstown, Ohio 44555, United States

Ibon Alkorta,* Goar Sánchez-Sanz, and José Elguero

Instituto de Química Médica (C.S.I.C.), Juan de la Cierva, 3, E-28006 Madrid, Spain

Supporting Information

ABSTRACT: Ab initio MP2/aug′-cc-pVTZ calculations have been carried out to investigate the influence of F−H···F hydrogen bonds on the P···N pnicogen bond in complexes nFH:(H_2FP:NFH_2) for n = 1−2, and a selected complex with n = 3. The NBO analysis indicates that the N(lp) → P−Fσ* charge-transfer transition has a much greater stabilizing effect than the P(lp) → N−Fσ* transition. When hydrogen bonding occurs at P−F, charge transfer associated with the pnicogen bond and the hydrogen bond are in the same direction but are in opposite directions when hydrogen bonding occurs at N−F. As a result, the formation of F−H···F hydrogen bonds at P−F leads to shorter P···N distances, increased strength of P···N bonds, and synergistic energetic effects; hydrogen bonding at N−F has opposite effects. ^{31}P and ^{15}N chemical shieldings do not correlate with charges on P and N, respectively, but ^{31}P shieldings correlate quadratically with the P−N distance. ^{1p}J(P−N) coupling constants do not correlate with the intermolecular P−N distance. However, when hydrogen bonding occurs only at P−F, ^{1p}J(P−N) decreases in absolute value as the P−N distance decreases, thereby approaching ^{1}J(P−N) for H_2P−NH_2. However, the P···N bond in 3FH:(H_2FP:NFH_2) has little covalent character, unlike the P···P bond in the corresponding complex 3FH:$(PH_2F)_2$.

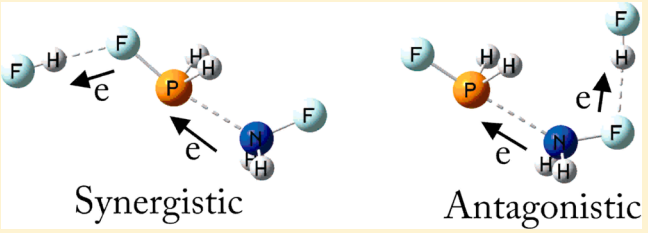

INTRODUCTION

The newest member of an ever-expanding list of intermolecular interactions is the pnicogen bond, a Lewis acid−Lewis base attractive interaction in which a pnicogen atom (N, P, or As) acts as the Lewis acid. In this respect, the pnicogen bond is analogous to some of the more familiar intermolecular interactions such as the hydrogen bond and the halogen bond. Beginning with the work of Hey-Hawkins et al.,[1] the pnicogen bond has received considerable attention in the recent literature.[2−20] In our most recent article in this area, we asked for the first time what effect F−H···F hydrogen bond formation at one or both P−F bonds in complexes nFH:$(PFH_2)_2$ would have on the strength of the P···P interaction.[20] We observed that hydrogen bonding strengthens the P···P bond, decreases the P−P distance, and alters other properties of these complexes, with the magnitude of the changes depending on the number of FH molecules and their positions in the complex.

In the parent molecule $(PH_2F)_2$, both PH_2F molecules are equivalent. On the basis of an NBO analysis, the dominant interaction in this complex is charge transfer from the lone pair on P in one molecule to the P−F sigma antibonding orbital of the other. However, forming one F−H···F hydrogen bond with one of the PH_2F molecules makes the two inequivalent, so that the stabilizing charge transfer interaction is favored in one direction over the other. That is, by making the two molecules inequivalent, we define which molecule acts as the acid and which is the base. We observed that the favored charge transfer interaction is that which involves the lone pair on the P atom of the molecule that is not hydrogen-bonded (the base) to the P−Fσ* orbital of the other molecule, which is involved in the F−H···F hydrogen bond (the acid).

It is appropriate to now ask what effect would F−H···F hydrogen bonding have if the two molecules involved in the pnicogen bond are not equivalent, as in (H_2FP:NFH_2), in which case the acid and the base are easily identified. To answer this question, we have investigated the P···N pnicogen bond in complexes nFH:(H_2FP:NFH_2), for n = 1 and 2, and in a selected complex 3FH:(H_2FP:NFH_2). In this article, we examine the structures of these complexes, their binding energies, the bonding characteristics of the P···N interaction, and the NMR properties of ^{31}P and ^{15}N chemical shieldings and ^{31}P−^{15}N spin−spin coupling constants. Our focus is on the effect of F−H···F hydrogen bonds at P−F and N−F on the properties of the P···N pnicogen bond.

METHODS

The structures of complexes nFH:PFH_2, nFH:NFH_2, and nFH:(H_2FP:NFH_2) for n = 1−2 and a selected complex 3FH:(H_2FP:NFH_2) were optimized at second-order Møller−Plesset

Received: August 14, 2012
Published: August 29, 2012

   dx.doi.org/10.1021/jp307083g | J. Phys. Chem. A 2012, 116, 9205−9213

perturbation theory (MP2)[21−24] with the aug′-cc-pVTZ basis set,[25] which is the Dunning aug-cc-pVTZ basis set[26,27] with diffuse functions removed from H atoms. Frequencies were computed to identify equilibrium and transition structures. One structure needed for energetic comparison was optimized with constraints and will be discussed below. All optimization calculations were performed using the Gaussian09 program.[28]

The electron densities of complexes have been analyzed employing the Atoms in Molecules (AIM) methodology[29,30] with the AIMAll program.[31] The Natural Bond Orbital (NBO) method[32] has been employed to compute atomic charges and to analyze charge-transfer interactions between occupied and virtual orbitals using the NBO-5 program[33] within the Gamess program.[34] The TOPMOD program[35] has been used to analyze the areas of electron concentration in terms of the Electron Localization Function (ELF).[36]

MP2/aug′-cc-pVTZ absolute chemical shieldings have been calculated within the GIAO approximation.[37] Coupling constants were evaluated using the equation-of-motion coupled cluster singles and doubles (EOM-CCSD) method in the configuration interaction (CI)-like approximation,[38,39] with all electrons correlated. For these calculations, the Ahlrichs[40] qzp basis set was placed on ^{19}F and ^{15}N, and the qz2p basis set on ^{31}P and the hydrogen-bonded ^{1}H atoms of FH molecules. The Dunning cc-pVDZ basis set was placed on the H atoms bonded to P and N. Only one-bond ^{31}P−^{15}N coupling constants across the pnicogen bond are reported in this article. It was demonstrated previously that the Fermi-contact term (FC) is by far the dominant term for P−P and P−N coupling and is an excellent approximation to total J in pnicogen dimers $(PH_2X)_2$[13] and $(PFHX)_2$[18,19] and in complexes $(H_2XP{:}NXH_2)$.[14] The FC term will be used to approximate ^{1p}J(P−N). The EOM-CCSD calculations were performed using ACES II[41] on the IBM Cluster 1350 (Glenn) at the Ohio Supercomputer Center.

RESULTS AND DISCUSSION

The results of this study have been subdivided into five sections. The first section presents a summary of the complexes nFH:NH_2F and nFH:$(H_2FP{:}NFH_2)$ and their designations. The second section provides a discussion of the geometries of these complexes, the binding energies of the P···N bond, and nonadditivity effects on complex binding energies. The third section presents the electronic properties of the complexes as described by AIM, NBO, and ELF methodologies. In the fourth section, the interplay between pnicogen bonds and hydrogen bonds is examined. In the fifth section, computed NMR ^{31}P and ^{15}N chemical shieldings and ^{31}P−^{15}N spin−spin coupling constants are discussed. In these sections, special attention is given to the effect of the presence of one or more F−H···F hydrogen bonds on the properties of the P···N pnicogen bond.

General Description of Complexes. Possible positions of the FH molecule acting as a hydrogen-bond donor to an F atom of PH_2F and NH_2F have been denoted as A, B, C, and D when hydrogen bonding occurs at P−F, and A′, B′, C′, and D′ when hydrogen bonding occurs at N−F, as illustrated in Scheme 1. A and B are *cis* and *trans*, respectively, to the bisector of the H−P−H angle, while C and D are essentially perpendicular to the plane defined by the bisector of this angle and the P−F bond. Similarly, A′ and B′ are *cis* and *trans*, respectively, to the bisector of the H−N−H angle, while C′ and D′ are essentially perpendicular to the plane defined by this bisector and the N−F bond.

Scheme 1. Positions of FH Molecules Interacting with the Binary Complex $(H_2FP{:}NFH_2)$

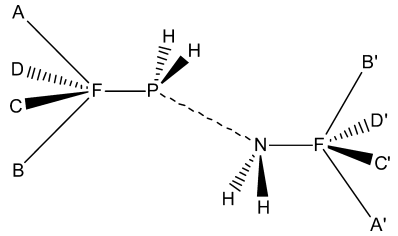

In addition to the A, B, C, and D designations to indicate the positions of the FH molecules, a second field has been used to indicate the number of molecules in the cluster. Thus, b, t, q, and p correspond to binary, ternary, quaternary, and penternary (quinternary) clusters, respectively. For example, tB′C′ corresponds to the $2FH{:}NH_2F$ complex with one of the FH molecules interacting with F at position B′ and the other at C′. qCD corresponds to the $2FH{:}(H_2FP{:}NFH_2)$ complex with FH molecules interacting with the F atom of PH_2F at positions C and D. qAC′ corresponds to the quaternary complex with one FH interacting with the F atom of PH_2F in position A and the other FH interacting with the F atom of NH_2F in position C′. These complexes are illustrated in Figures 1 and 2.

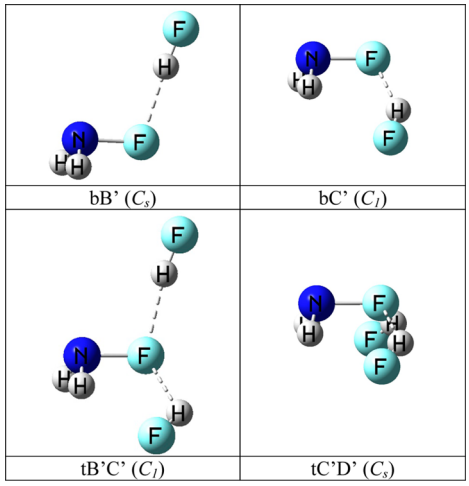

Figure 1. Structures of complexes $FH{:}NFH_2$ and $2FH{:}NFH_2$.

The nFH:PH_2F complexes have been described in a previous article[20] and will not be discussed further here. Two equilibrium $FH{:}NFH_2$ binary complexes bB′ (21.5 kJ/mol) and bC′ (22.3 kJ/mol) have been found on the potential surface, and these are illustrated in Figure 1. A complex bA′ has been optimized, but it is not an equilibrium structure and converts to bC′. In bC′, the hydrogen-bonded FH is oriented such that the F of FH also interacts with one of the H atoms of NH_2F. However, this secondary interaction is relatively weak, and no bond critical point (BCP) is indicated in the AIM analysis.

Two $2FH{:}NH_2F$ equilibrium structures have been found, and these are also illustrated in Figure 1. In the first tB′C′ (37.9 kJ/mol), the orientations of the FH molecules are similar to the orientations found in bB′ and bC′. The second equilibrium structure, tC′D′ (38.2 kJ/mol), has C_s symmetry with the FH

dx.doi.org/10.1021/jp307083g | J. Phys. Chem. A 2012, 116, 9205−9213

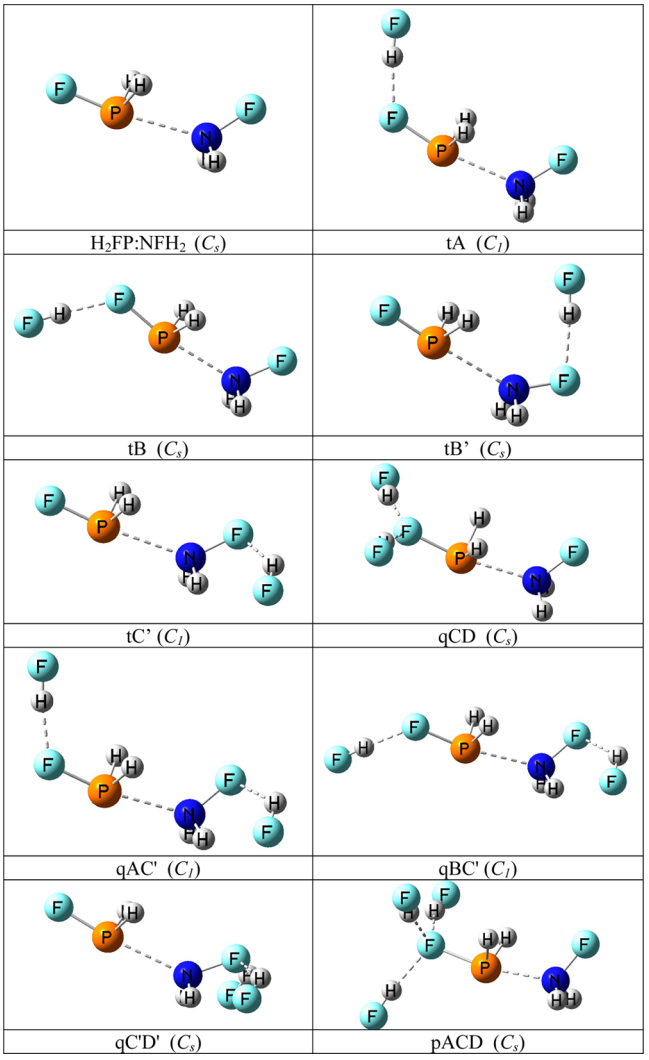

Figure 2. Structures of complexes FH:(H_2FP:NFH_2), 2FH:(H_2FP:NFH_2), and the single complex 3FH:(H_2FP:NFH_2).

molecules oriented as in bC′, with one FH above the symmetry plane of the complex and the other below.

Four equilibrium structures have been found for complexes with one FH molecule bonded to (H_2FP:NFH_2) and four for complexes with two FH molecules bonded to (H_2FP:NFH_2). These are illustrated and given designations in Figure 2. Additional searches of the potential surfaces for complexes with one or two FH molecules interacting with (H_2FP:NFH_2) were carried out both with and without symmetry, but no other equilibrium structures were found.

In ref 20, we described in detail the interesting and unusual characteristics of the complex in which three FH molecules are hydrogen bonded to the same P−F bond in 3FH:$(PH_2F)_2$. (This structure was designated pACC in ref 20 but to be consistent with the coding used in the present study, it is pACD.) Therefore, we have included the corresponding complex 3FH:H_2FP:NFH_2 (pACD) with three FH molecules hydrogen-bonded to the F atom of PH_2F. Needed for energetic comparison is the quaternary complex 3FH:PFH_2 (qACD), which is not an equilibrium structure on its potential surface. Therefore, a constrained optimization was carried out in which the P−F−F angle was fixed at its value in the penternary complex to prevent migration of FH toward P, and the remaining coordinates were optimized. Complex pACD is illustrated in Figure 2.

Structures and Binding Energies. *Structures.* The geometries of complexes *n*FH:NFH_2 and *n*FH:(H_2FP:NFH_2) with n = 1 and 2, and the single structure with n = 3 are reported in Table S1 of the Supporting Information and illustrated in Figures 1 and 2, respectively, where they are identified by their code. Table 1 reports the P−N distances in these complexes. In complexes FH:(H_2FP:NFH_2), hydrogen bond formation at the P−F bond in tA and tB decreases the P−N distance by about 0.127 Å, in agreement with the trend observed for hydrogen-bond formation in complexes *n*FH:$(PH_2F)_2$.[20] In contrast, hydrogen bond formation at the N−F bond leads to a lengthening of the P−N distance by 0.075 Å in tB′ and 0.022 Å in tC′.

The 2HF:(H_2FP:NFH_2) complexes can be subdivided into three different groups: (i) complex qCD in which the two HF molecules interact with the PH_2F molecule. In this complex, the P−N distance decreases by 0.269 Å, which is slightly more than twice that observed for tA and tB; (ii) two complexes with one FH molecule hydrogen bonded to P−F and the second to N−F (qAC′ and qBC′). These complexes have P−N distances slightly greater than tA and tB; (iii) complex qC′D′ with both FH molecules hydrogen-bonded to N−F. In this complex, the P−N distance decreases relative to tB′ and tC′ but is 0.008 Å longer than the P−N distance in the parent complex (H_2FP:NFH_2). Thus, it appears that hydrogen-bond formation at P−F always leads to a shortening of the P−N distance, with the shortening increasing as the number of FH molecules increases. In contrast, hydrogen-bond formation at N−F tends to lengthen the P−N bond, but the changes are smaller than changes in this bond length when hydrogen bonding occurs at

Table 1. P−N, P−F, and N−F Distances (Å) in Complexes *n*FH:PFH_2, *n*FH:NFH_2, and *n*FH:(H_2FP:NFH_2)

	FH at P−F			same no. of FH at P−F and N−F			FH at N−F		
complex	P−N	P−F	N−F	P−N	P−F	N−F	P−N	P−F	N−F
(H_2FP:NFH_2)				2.524	1.638	1.420			
tA	2.398	1.678	1.415						
tB	2.397	1.677	1.416						
tB′							2.599	1.629	1.435
tC′							2.546	1.635	1.434
qCD	2.255	1.732	1.411						
qAC′				2.401	1.677	1.425			
qBC′				2.401	1.675	1.427			
qC′D′							2.532	1.634	1.445
pACD	2.143	1.800	1.407						

dx.doi.org/10.1021/jp307083g | J. Phys. Chem. A 2012, 116, 9205−9213

P−F. Not surprisingly, complex pACD with three FH molecules hydrogen bonded to P−F has the shortest P−N distance of 2.143 Å. However, this distance is significantly longer than the P−N distance of 1.725 Å computed at the same level of theory for the H_2P-NH_2 molecule. The significance of this difference will be discussed below.

It is not surprising that hydrogen-bond formation also leads to changes in P−F distances, an observation first made for the P−F distance in complexes nHF:$(PH_2F)_2$.[20] P−F and N−F bond distances are also reported in Table 1. P−F bond distances increase relative to the parent complex when hydrogen bonding occurs at P−F, with the degree of lengthening increasing as the number of F−H···F hydrogen bonds increases. From Table 1, it can be seen that the P−N, P−F, and N−F distances in qAC′ and qBC′ are very similar to the corresponding distances in tA and tB, again suggesting that the these distances are sensitive to the number of F−H···F hydrogen bonds at P−F and not very sensitive to hydrogen bonding at N−F. A good correlation exists between the P−N and P−F distances in these complexes, as illustrated in Figure 3.

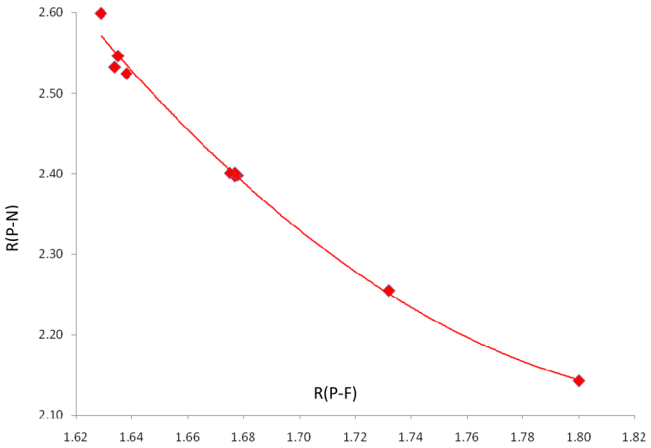

Figure 3. P−N vs P−F distances (Å). The correlation coefficient R^2 = 0.992.

When hydrogen bonding occurs at N−F, the P−F bond shortens slightly. The N−F bond tends to lengthen with hydrogen bond formation at N−F but shorten when bonding occurs at P−F. However, the changes in the length of the N−F bond are much less than those found for the P−F bond.

Binding Energies. In order to assess the effect of hydrogen bond formation at F on the strength of the P···N pnicogen bond, binding energies of complexes nFH:$(H_2FP:NFH_2)$ have been computed relative to the energies of the two fragments that form the P···N bond. By using complexes tA and qAC′ as examples, we obtain

$$\Delta E(\mathrm{tA}) = -[E(\mathrm{tA}) - E(\mathrm{bA}) - E(\mathrm{NFH_2})] \quad (1)$$

$$\Delta E(\mathrm{qAC'}) = -[E(\mathrm{qAC'}) - E(\mathrm{bA}) - E(\mathrm{bC'})] \quad (2)$$

Thus, the binding energy of the P···N bond is the negative of the reaction energy for the formation of the complex. The computed P···N binding energies are reported in Table 2.

From Table 2, it can be seen that hydrogen bond formation only at P−F increases the energy of the P···N bond relative to the parent complex $(H_2FP:NFH_2)$. The binding energies increase as the number of FH molecules increases and range from 34 to 57 kJ/mol, compared to 27 kJ/mol for the parent

Table 2. Binding Energies (ΔE, kJ/mol) of Complexes nFH:PFH_2, nFH:NFH_2, and nFH:$(H_2FP:NFH_2)$

complex	FH at P−F	same no. of FH at P−F and N−F	FH at N−F
$H_2FP:NFH_2$		26.67[a]	
tA	34.37		
tB	35.29		
tB′			22.60
tC′			23.69
qCD	45.20		
qAC′		30.64	
qBC′		31.10	
qC′D′			23.18
pACD	56.83		

[a]Reference 14.

complex. In contrast, the energy of the P···N bond decreases when FH molecules hydrogen bond at N−F. This decrease is not very sensitive to the number of FH molecules present, as these binding energies are approximately 23 kJ/mol. The binding energies of complexes qAC′ and qBC′ are 31 kJ/mol, intermediate between tA and tB (35 kJ/mol) and tB′ and tC′ (23 kJ/mol).

An estimate of the average effect of hydrogen bond formation on the strength of the P···N bond can be obtained from eq 3

$$\Delta E(\mathrm{P\cdots N}) = (25.4 \pm 1.2) + (9.9 \pm 0.7)[(n_\mathrm{P}(\mathrm{P-F})] - (2.2 \pm 1.0)[n_\mathrm{N}(\mathrm{N-F})] \quad (3)$$

with n = 10, R^2 = 0.97, SD = 1.6, and n_P and n_N equal to the number of hydrogen bonds at P−F and N−F, respectively. Each hydrogen bond formed at P−F strengthens the P···N interaction by about 10 kJ/mol. In contrast, formation of a hydrogen bond at N−F weakens the P···N bond by 2 kJ/mol. The constant in eq 3 approximates the value of the binding energy of the parent binary complex $(H_2FP:NFH_2)$.

Since the complexes nFH:$(H_2FP:NFH_2)$ are stabilized by two different types of intermolecular interactions, we have also evaluated the cooperative effect (nonadditivity) of the interaction energies using eq 4

$$\delta\Delta E = -\{\Delta E[n\mathrm{FH}:(H_2FP:NFH_2)] - \Sigma_i \Delta E_i(\mathrm{binary})\} \quad (4)$$

with $\Delta E[n$FH:$(H_2FP:NFH_2)]$ being the total binding energy of the complex relative to the corresponding isolated monomers, and $\Sigma_i \Delta E_i$(binary) being the sum of the binding energies of all binary interactions in the complex. The nonadditivities are reported in Table 3. From these data, it is apparent that binding energies are nonadditive in a positive sense, that is, they are synergistic, when hydrogen bond formation occurs at the P−F bond. For these, the cooperative effect ranges from 7.7 kJ/mol for tA to 12.5 kJ/mol for qCD. This is quite different from the nonadditivities found for the nFH:$(PH_2F)_2$ complexes, for which a significantly greater synergistic effect was found for pACD. In contrast, when hydrogen bonding occurs at N−F, binding energies are nonadditive in a negative sense, that is, they are diminutive. Nonadditivities range from −3.0 kJ/mol for tC′ to −9.9 kJ/mol for qC′D′.

AIM, ELF, and NBO analyses. The topological analysis of the electron density shows the presence of intermolecular bond critical points (BCPs) and corresponding bond paths connecting the pnicogen-bonded P···N atoms and the hydrogen-bonded H···F atoms. The molecular graphs of the

dx.doi.org/10.1021/jp307083g | J. Phys. Chem. A 2012, 116, 9205−9213

Table 3. Nonadditivities of Interaction Energies ($\delta\Delta E$, kJ/mol)[a] for Complexes nFH:(H_2FP:NFH_2)

complex	FH at P−F	same no. of FH at P−F and N−F	FH at N−F
tA	7.70		
tB	8.62		
tB′			−4.70
tC′			−2.98
qCD	12.51		
qAC′		3.97	
qBC′		4.43	
qC′D′			−9.86
pACD	9.21		

[a] $\delta\Delta E = -\{\Delta E[n\text{FH:}(H_2\text{FP:N}FH_2)] - \Sigma_i \Delta E_i(\text{binary})\}$.

complexes are shown in the Supporting Information. Electron densities at BCPs (ρ_{BCP}) are reported in Table S2 of the Supporting Information. Values of ρ_{BCP} increase as intermolecular distances decrease. The plot of these two variables appears as Figure S2 of the Supporting Information and shows an excellent exponential relationship, in agreement with previous findings for intermolecular interactions.[42−48]

The values of the Laplacian of the electron density at the BCP ($\nabla^2\rho_{BCP}$),[49] the total energy density at the BCP (H_{BCP}),[50] and the ratio of the absolute value of the electron potential energy density to the kinetic energy density ($C = |V|/G$)[51] have been computed and used to assess the degree of covalency of the P···N interaction. In all complexes nFH:(H_2FP:NFH_2), the Laplacians are positive, the total energy densities are negative but usually very small, and C values are always less than 2. The values of these three variables are clear indications that the P···N interaction in these complexes has little covalency. Only the complex pACD with the shortest P···N distance has a value of the Laplacian that is close to zero and the largest value of C at 1.855. Thus, this complex has the highest degree of covalency, even though its covalent character is small. The degree of covalency in the complexes nFH:(H_2FP:NFH_2) is dramatically different from that in complexes nFH:$(PH_2F)_2$, all of which have some degree of covalent character.[20] The covalent character of the P···P bond in 3FH:$(PH_2F)_2$ (qACD) is significant, as the P−P distance approaches the value of the P−P distance in H_2P-PH_2.

The ELF representation of complexes nFH:(H_2FP:NFH_2) clearly indicates that the lone pair on the nitrogen is directed toward the P···N region, while the lone pair on phosphorus is not. The electrons in the intermolecular region are assigned to a P−N basin only in complexes in which hydrogen bonding with FH occurs at P−F. This is illustrated in Figure 4 for the complex pACD. When hydrogen bonding occurs at N−F, electrons in the P−N region are described as nitrogen lone pairs.

When the default parameters for the NBO analysis are used to analyze nFH:(H_2FP:NFH_2) complexes with hydrogen-bond formation at P−F, the NBO method usually describes the (H_2FP:NFH_2) binary complex as a molecule with a formal P−N bond. This description parallels the assignment of the electrons in this region to the P−N basin in the ELF analysis. In order to quantify the orbital interaction energies between PH_2F and NH_2F, it was necessary to impose a Lewis structure with no P−N bond. The resulting orbital interaction energies are reported in Table 4. In the parent complex (H_2FP:NFH_2), both NFH_2 and PFH_2 have lone pairs of electrons, so both may act as electron-pair donors. However, since NFH_2 is the stronger

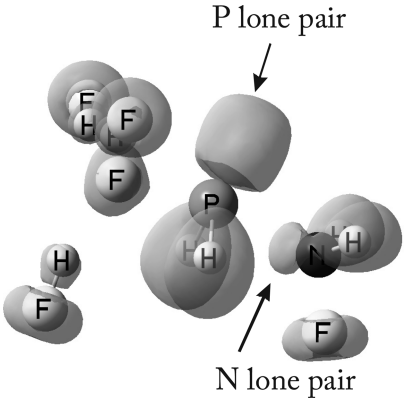

Figure 4. ELF at 0.8 isosurface for pACD complex.

base, it would be expected to be the electron-pair donor. Thus, Table 4 shows that the stabilizing charge-transfer orbital interaction energy for N(lp) → P−Fσ* is significantly greater than the energy for P(lp) → N−Fσ*. This is also consistent with the results of the ELF analysis.

What effect does hydrogen-bond formation have on orbital interaction energies? As evident from Table 4, formation of F−H···F hydrogen bonds at P−F significantly increases the N(lp) → P−Fσ* interaction energy, from 59 kJ/mol in the parent molecule to 91 kJ/mol for tA and tB, 137 kJ/mol for qCD, and 195 kJ/mol for pACD. In contrast, this interaction energy decreases from 59 kJ/mol in (H_2FP:NFH_2) to between 44 and 54 kJ/mol when hydrogen bonding occurs at N−F in complexes tB′, tC′, and qC′D′. When hydrogen bond formation occurs at both P−F and N−F, the N(lp) → P−Fσ* interaction energies for qAC′ and qBC′ are very close to the values for tA and tB at 90 kJ/mol. Thus, it is apparent that the N(lp) → P−Fσ* excitation is very sensitive to hydrogen bond formation, increasing if hydrogen bonding occurs at P−F and at both P−F and N−F but decreasing if it occurs only at N−F.

The P(lp) → N−Fσ* orbital interaction energy is much less sensitive to the number and positions of FH molecules. Thus, when hydrogen bonding occurs at P−F, this energy decreases from 12 kJ/mol in the parent molecule to 9 kJ/mol when only one hydrogen bond is present, is equal to 12 kJ/mol when two hydrogen bonds are formed, and increases to 15 kJ/mol in pACD. When hydrogen bonding occurs at N−F, the P(lp) → N−Fσ* energies vary from 14 to 16 kJ/mol, and when hydrogen bonds are formed at P−F and N−F, the interaction energies are 9 and 10 kJ/mol.

Interplay of Pnicogen Bonding and Hydrogen Bonding. There are two different intermolecular interactions that stabilize the complexes nFH:(H_2FP:NFH_2), namely, the pnicogen bond and the hydrogen bond. How do these interplay? Some insight into the answer to this question can be gained by using the electron densities in Tables S3 and S4, Supporting Information, to examine charge transfer in the binary complexes FH:PFH_2 (bB) and FH:NFH_2 (bB′), the parent complex (H_2FP:NFH_2), and the two ternary complexes FH:(H_2FP:NFH_2) (tB and tB′).

As evident from Table S4, Supporting Information, in complexes bB and bB′, charge transfer occurs from the base, PH_2F and NH_2F, respectively, to the proton-donor molecule FH, as expected. In the parent complex (H_2FP:NFH_2), charge transfer occurs from the base NFH_2 to the acid PFH_2, so that NFH_2 becomes slightly positively charged and PFH_2 becomes

dx.doi.org/10.1021/jp307083g | J. Phys. Chem. A 2012, 116, 9205−9213

Table 4. NBO P(lp) → N−Fσ* and N(lp) → P−Fσ* Orbital Interaction Energies (kJ/mol)

	P(lp) → N−Fσ*			N(lp) → P−Fσ*		
complex	FH at P−F	same no. FH at each	FH at N−F	FH at P−F	same no. FH at each	FH at N−F
$H_2FP{:}NFH_2$		12.3			58.7	
tA	9.1			91.3		
tB	9.5			91.4		
tB′			15.4			43.5
tC′			13.9			53.5
qCD	12.0			137.2		
qAC′		9.2			90.3	
qBC′		9.9			89.9	
qC′D′			15.9			54.5
pACD	15.3			195.2		

slightly negatively charged (+0.048e and −0.048e). This direction of charge transfer is also consistent with the observation that N(lp) → P−Fσ* is by far the dominant stabilizing charge-transfer transition, being much more important that P(lp) → N−Fσ*. Moreover, in the parent complex, P gains 0.060 electrons while N also gains 0.014 electrons. Since N gains electron density at the same time that NH_2F loses electron density, there must also be donation from the P lone pair to the N [P(lp) → N−Fσ*]. Nevertheless, since P gains more density (0.060e) than the PH_2F molecule (0.048e), the N(lp) → P−Fσ* charge-transfer transition must be dominant, consistent with the data of Table 4.

How charge transfer occurs in tB and tB′ provides insight into the interplay of pnicogen bonding and hydrogen bonding. When hydrogen bonding occurs at P−F (tB), there is little change in the charges on P and N, even though the N(lp) → P−Fσ* excitation is even more stabilizing than in the parent complex. However, electron density is lost by NH_2F (0.030e) and gained by PH_2F (0.010e) and by FH (0.020e). Charge-transfer occurs from the nonhydrogen-bonded NH_2F molecule to the hydrogen-bonded PH_2F molecule and to FH. Thus, charge transfer in tB is in the same direction as in the parent complex ($H_2FP{:}NFH_2$). This results in an increased stability of tB relative to the parent.

When hydrogen bonding occurs at N−F (tB′), the positive charge on P increases by 0.004e and the negative charge on N also increases by 0.005e. Relative to the parent complex, the N(lp) → P−Fσ* excitation is less stabilizing by 15.2 kJ/mol while the P(lp) → N−Fσ* excitation is more stabilizing by 3.1 kJ/mol. At the same time, PH_2F loses 0.033 electrons, while NH_2F gains 0.016 electrons and FH gains 0.017 electrons. Thus, charge transfer again occurs from the nonhydrogen-bonded PFH_2 molecule to the hydrogen-bonded NFH_2 molecule and to FH, but this is in the opposite direction from the parent complex. That is, this is not the preferred direction for the pnicogen bond, with the result that hydrogen bonding at N−F decreases the stability of the P···N bond. Thus, it appears that in these complexes, hydrogen-bonding is the dominant intermolecular interaction. When hydrogen bonding occurs at P−F, the direction of charge flow is that preferred in the parent complex, the complexes are more stable than the parent, and nonadditivities are synergistic. In contrast, when hydrogen bonding occurs at N−F, the direction of charge flow is opposite to that preferred in the parent complex, the complexes are less stable, and nonadditivities are antagonistic.

NMR Properties. *Chemical Shieldings.* ^{31}P and ^{15}N chemical shieldings are reported in Table 5. Since hydrogen bonding at P−F reduces the positive charge on P, the ^{31}P chemical shielding increases as the number of hydrogen bonds at P−F increases, from 340 ppm in the parent molecule, to 360, 385, and 406 ppm in complexes with one, two, and three FH molecules, respectively. At the same time, the negative charge on N decreases, but the decrease does not correlate with the small increase in the ^{15}N chemical shielding from 80 ppm in the parent complex to 82, 85, and 89 ppm as the number of hydrogen-bonded FH molecules increases.

Table 5. ^{31}P and ^{15}N Absolute Chemical Shieldings (ppm)

	FH at PH_2F		same number of FH at P−F and N−F		FH at NH_2F	
	^{15}N	^{31}P	^{15}N	^{31}P	^{15}N	^{31}P
$(H_2FP{:}NFH_2)$			79.9	339.7		
tA	82.6	360.4				
tB	82.2	357.9				
tB′					66.8	316.5
tC′					64.5	332.2
qCD	85.0	384.9				
qAC′			71.2	359.4		
qBC′			70.1	355.4		
qC′D′					51.0	332.4
pACD	88.8	406.0				

Not surprisingly, relative to the parent complex, charges on atoms and chemical shifts change very little in qAC′ and qBC′ when hydrogen bonding occurs at both P−F and N−F sites. When hydrogen bonding occurs only at N−F, the positive charge on P and the negative charge on N both increase. Although the ^{31}P chemical shielding does decrease relative to ($H_2FP{:}NFH_2$), the smallest shielding is found in tB′. However, the ^{15}N chemical shielding decreases and has its smallest value in qC′D′, which does not correlate with the electron density changes at N.

For all of the complexes with P···N bonds investigated in this study, the ^{31}P chemical shielding exhibits a surprisingly clear relationship with the intermolecular P···N distance. Figure 5 presents a plot of the ^{31}P chemical shielding as a function of the P−N distance for these complexes, and including the covalently bonded $H_2P{-}NH_2$ molecule. An unanticipated, yet excellent second order relationship, is obtained between these two variables, with a correlation coefficient R^2 of 0.995.

$^{31}P{-}^{15}N$ Spin−Spin Coupling Constants. In ref 14, we demonstrated that the FC term is an excellent approximation to total ^{1p}J(P−N). Hydrogen bonding of an FH molecule in complexes tA, tB, and tB′ does not change this situation. For these complexes, the difference between the FC term and total

dx.doi.org/10.1021/jp307083g | J. Phys. Chem. A 2012, 116, 9205−9213

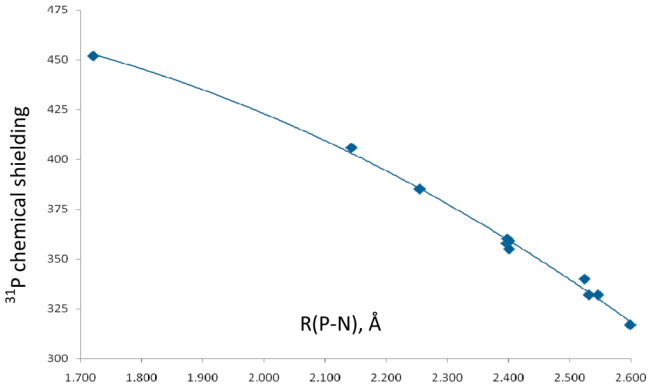

Figure 5. ^{31}P Chemical shielding (ppm) vs P−N interatomic distance (Å).

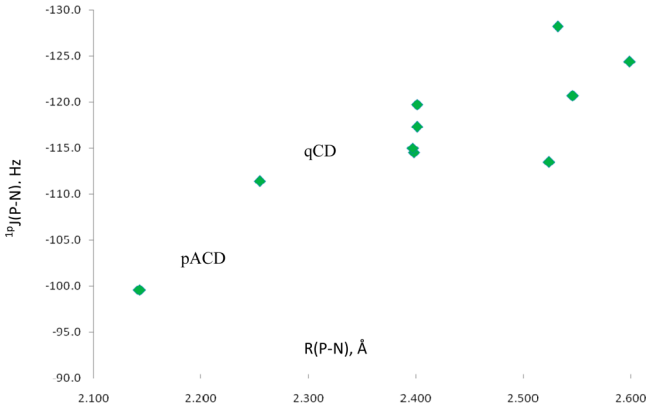

Figure 6. ^{1p}J(P−N) vs the P−N distance.

^{1p}J(P−N) does not exceed 0.2 Hz for coupling constants that are greater than 100 Hz. Thus, the FC term will again be used to approximate total J.

Table 6 provides intermolecular P−N distances and values of ^{1p}J(P−N), and Figure 6 presents a scattergram of these data. Similar to ^{1p}J(P−P) for complexes nFH:$(PH_2F)_2$, ^{1p}J(P−N) does not exhibit a systematic dependence on the P−N distance. Relative to the parent molecule, which has a P−N distance of 2.524 Å and ^{1p}J(P−N) equal to −113.5 Hz, hydrogen bonding of FH at P−F in tA and tB leads to a significant decrease in the P−N distance of about 0.13 Å, but ^{1p}J(P−N) increases only slightly by 1.0 and 1.5 Hz, respectively. In contrast, hydrogen bonding of one FH molecule to N−F leads to an increase in the P−N distance of 0.075 and 0.022 Å in tB′ and tC′, respectively, but ^{1p}J(P−N) also increases by 11 and 7 Hz, respectively.

In complex qCD, which has both FH molecules hydrogen bonded to P−F, the P−N distance further decreases to 2.255 Å, but ^{1p}J(P−N) also decreases by about 3 Hz relative to tA and tB. In contrast, bonding both FH to N−F leads to a P−N distance that is similar to that in $(H_2FP{:}NFH_2)$, but ^{1p}J(P−N) has its largest absolute value of −128.1 Hz. When P−F and N−F are each hydrogen-bonded to one F−H molecule, the P−N distance has a value similar to that found for tA and tB and ^{1p}J(P−N) values that are intermediate between qCD and qC′D′.

Perhaps the most interesting result is the value of ^{1p}J(P−N) for the penternary complex pACD. Although the P−N distance is shortest in this complex, ^{1p}J(P−N) has its smallest absolute value of −99.6 Hz. The lack of a correlation between R(P−N) and ^{1p}J(P−N) is clearly demonstrated in Figure 6. To gain insight into this behavior, it is advantageous to consider the situation for the corresponding complex 3FH:$(PH_2F)_2$ with all three FH molecules bonded to the same P−F.[20] For this complex, the P−F distance lengthens by 0.21 Å, and the three FH molecules hydrogen bonded to F resemble an anionic cluster $3(FH)F^-$ with approximately local C_{3v} symmetry. As the complex approaches an ion-pair complex $3(HF)F^-$:$(H_2P{:}PFH_2)^+$, the P−P distance shortens to a value that is only 0.135 Å longer than the P−P bond in the C_{2v} structure of P_2H_4, and the P···P pnicogen bond has significant covalent character. As a result, ^{1p}J(P−P) approaches ^1J(P−P) for P_2H_4.

A similar situation occurs but to a much lesser extent in 3FH:$(H_2FP{:}NFH_2)$ (pACD). In this complex, the P−F bond lengthens by 0.16 Å, the three FH molecules hydrogen bonded to F show some resemblance to an anionic cluster $3(FH)F^-$ with approximately local C_{3v} symmetry, and the P−N bond shortens to 2.143 Å, thereby acquiring some covalent character. However, this bond length is significantly greater by 0.377 and 0.423 Å, respectively, than the computed MP2/aug-cc-pVTZ P−N bond length in the C_{2v} and C_1 structures of $H_2P{-}NH_2$. The FC terms for P−N coupling in these structures are 12.9 and 44.5 Hz, respectively. Thus, the FC term does decrease systematically in absolute value in complexes with 1, 2, and 3 FH molecules at P−F, and in qACD, it does appear to be approaching the value for the covalent bond in $H_2P{-}NH_2$. However, the differences between distances and coupling constants in qACD and $H_2P{-}NH_2$ are significant. Nevertheless, the decrease in ^{1p}J(P−N) in pACD is a reflection of the changing nature of the P−N pnicogen bond.

Table 6. R(P−N) (Å) and ^{1p}J(P−N) (Hz)[a] for Complexes nFH:$(H_2FP{:}NFH_2)$ with n = 1−3

	FH at PH_2F		same no. FH at each		FH at NH_2F	
complex	R(P−N)	^{1p}J(P−N)	R(P−N)	^{1p}J(P−N)	R(P−N)	^{1p}J(P−N)
$(H_2FP{:}NFH_2)$			2.524	−113.5		
tA	2.398	−114.5				
tB	2.397	−115.0				
tB′					2.599	−124.4
tC′					2.546	−120.7
qCD	2.255	−111.4				
qAC′			2.401	−117.3		
qBC′			2.401	−119.7		
qC′D					2.532	−128.2
pACD	2.143	−99.6				

[a]Approximated by the FC term.

dx.doi.org/10.1021/jp307083g | J. Phys. Chem. A 2012, 116, 9205−9213

CONCLUSIONS

Ab initio MP2/aug′-cc-pVTZ calculations have been carried out to investigate the effect of F−H···F hydrogen bonds on the P···N pnicogen bond in complexes nFH:(H_2FP:NFH_2) for n = 1 and 2 and a selected complex 3FH:(H_2FP:NFH_2). The following statements are based on the results of this study.

(1) The P−N distance decreases, the strength of the P···N pnicogen interaction increases, and complex binding energies are synergistic when F−H···F hydrogen bonds form at P−F. The extent of these changes scales with the number of hydrogen bonds.

(2) The P−N distance increases, the strength of the P···N pnicogen interaction decreases, and complex binding energies are diminutive when hydrogen bonding occurs at N−F. The extent of these changes is smaller than those observed when hydrogen bonding occurs at P−F.

(3) The NBO analysis indicates that the charge-transfer transition N(lp) → P−Fσ* is important for the stabilization of complexes nFH:(H_2FP:NFH_2). It is significantly more important for P···N bonding than the P(lp) → N−Fσ* transition.

(4) The NBO analysis indicates that charge transfer from N to P is favored for the pnicogen bond. For the hydrogen bond, charge transfer to FH is favored. When hydrogen bonding occurs at P−F, charge transfer associated with these two interactions is in the same direction. This leads to increased stability of the P···N bond and synergistic energetic effects. When hydrogen bonding occurs at N−F, charge transfer for the two interactions is in opposite directions, which leads to decreased stability of the P···N bond and diminutive energetic effects.

(5) Although ^{31}P chemical shieldings increase as the number of F−H bonds formed only at P−F increases, no correlation is found between ^{31}P and ^{15}N chemical shieldings and charges at P and N, respectively. However, ^{31}P chemical shieldings in complexes nFH:(H_2FP:NFH_2) correlate quadratically with the P−N distance.

(6) In general, ^{1p}J(P−N) does not correlate with the intermolecular P−N distance. However, when hydrogen bonding occurs only at P−F, ^{1p}J(P−N) decreases in absolute value as the P−N distance decreases. While its value in 3FH:(H_2FP:NFH_2) does appear to be approaching the value in the molecule H_2P−NH_2, the differences between distances and P−N coupling constants in these two moieties are significant. The P···N bond in the complex has little covalent character, unlike the P···P bond in the corresponding complex 3FH:(PH_2F)$_2$.

ASSOCIATED CONTENT

Supporting Information

MP2/aug′ccpVTZ structures and energies, electron density molecular graphs, electron density at the P···N BCP parameters, NBO charges on atoms and molecules, and full references 28, 34, and 41. This material is available free of charge via the Internet at http://pubs.acs.org.

AUTHOR INFORMATION

Corresponding Author

*E-mail: jedelbene@ysu.edu (J.E.D.B.); ibon@iqm.csic.es (I.A.).

Notes

The authors declare no competing financial interest.

ACKNOWLEDGMENTS

This work was carried out with financial support from the Ministerio de Educación y Ciencia (Project No. CTQ200913129C0202) and Comunidad Autónoma de Madrid (Project MADRISOLAR2, ref S2009/PPQ1533). Thanks are given to the Ohio Supercomputer Center for its continued support and to the CTI (CSIC) and CCC (UAM) for an allocation of computer time.

REFERENCES

(1) Zahn, S.; Frank, R.; Hey-Hawkins, E.; Kirchner, B. *Chem.—Eur. J.* **2011**, *17*, 6034−6038.
(2) Solimannejad, M.; Gharabaghi, M.; Scheiner, S. *J. Chem. Phys.* **2011**, *134*, 024312−024316.
(3) Scheiner, S. *J. Chem. Phys.* **2011**, *134*, 094315−094319.
(4) Scheiner, S. *J. Phys. Chem. A* **2011**, *115*, 11202−11209.
(5) Adhikari, U.; Scheiner, S. *J. Phys. Chem. A* **2012**, *116*, 3487−3497.
(6) Adhikari, U.; Scheiner, S. *Chem. Phys. Lett.* **2012**, *532*, 31−35.
(7) Scheiner, S. *Chem. Phys. Lett.* **2011**, *514*, 32−35.
(8) Scheiner, S. *Chem. Phys.* **2011**, *387*, 79−84.
(9) Scheiner, S. *J. Chem. Phys.* **2011**, *134*, 164313−164319.
(10) Adhikari, U.; Scheiner, S. *J. Chem. Phys.* **2011**, *135*, 184306−184315.
(11) Scheiner, S.; Adhikari, U. *J. Phys. Chem. A* **2011**, *115*, 11101−11110.
(12) Scheiner, S. *Phys. Chem. Chem. Phys.* **2011**, *13*, 13860−13872.
(13) Del Bene, J. E.; Alkorta, I.; Sánchez-Sanz, G.; Elguero, J. *Chem. Phys. Lett.* **2011**, *512*, 184−187.
(14) Del Bene, J. E.; Alkorta, I.; Sánchez-Sanz, G.; Elguero, J. *J. Phys. Chem. A* **2011**, *115*, 13724−13731.
(15) Adhikari, U.; Scheiner, S. *Chem. Phys. Lett.* **2012**, *536*, 30−33.
(16) Li, Q.-Z.; Li, R.; Liu, X.-F.; Li, W.-Z.; Cheng, J.-B. *J. Phys. Chem. A* **2012**, *116*, 2547−2553.
(17) Li, Q.-Z.; Li, R.; Liu, X.-F.; Li, W.-Z.; Cheng, J.-B. *ChemPhysChem* **2012**, *13*, 1205−1212.
(18) Del Bene, J. E.; Alkorta, I.; Sánchez-Sanz, G.; Elguero, J. *J. Phys. Chem. A* **2012**, *116*, 3056−3060.
(19) Del Bene, J. E.; Alkorta, I.; Sánchez-Sanz, G.; Elguero, J. *Chem. Phys. Lett.* **2012**, *538*, 14−18.
(20) Alkorta, I.; Sánchez-Sanz, G.; Elguero, J.; Del Bene, J. E. *J. Chem. Theory Comp.* **2012**, *8*, 2320−2327.
(21) Pople, J. A.; Binkley, J. S.; Seeger, R. *Int. J. Quantum Chem.* **1976**, *10*, 1−19.
(22) Krishnan, R.; Pople, J. A. *Int. J. Quantum Chem.* **1978**, *14*, 91−100.
(23) Bartlett, R. J.; Silver, D. M. *J. Chem. Phys.* **1975**, *62*, 3258−3268.
(24) Bartlett, R. J.; Purvis, G. D. *Int. J. Quantum Chem.* **1978**, *14*, 561−581.
(25) Del Bene, J. E. *J. Phys. Chem.* **1993**, *97*, 107−110.
(26) Dunning, T. H. *J. Chem. Phys.* **1989**, *90*, 1007−1023.
(27) Woon, D. E.; Dunning, T. H. *J. Chem. Phys.* **1995**, *103*, 4572−4585.
(28) Frisch, M. J.; Trucks, G. W.; Schlegel, H. B.; Scuseria, G. E.; Robb, M. A.; Cheeseman, J. R.; Scalmani, G.; Barone, V.; Mennucci, B.; Petersson, G. A.; et al. *Gaussian 09*, revision A.02; Gaussian, Inc.: Wallingford, CT, 2009.
(29) Bader, R. F. W.; Halpen, J.; Green, M. L. H. *Atoms in Molecules: A Quantum Theory*, Clarendon Press: Oxford, U.K., 1990.
(30) Popelier, P. L. A. *Atoms in Molecules: An Introduction*; Pearson Education Limited: Essex, U.K., 2000.
(31) Keith, T. A. *AIMAll*; TK Gristmill Software: Overland Park, KS, 2011; see aim.tkgristmill.com.
(32) Reed, A. E.; Curtiss, L. A.; Weinhold, F. *Chem. Rev.* **1988**, *88*, 899−926.

(33) Glendening, E. D.; Badenhoop, J. K.; Reed, A. E.; Carpenter, J. E.; Bohmann, J. A.; Morales, C. M.; Weinhold, F. *NBO 5.G*; University of Wisconsin: Madison, WI, 2004.
(34) Schmidt, M. W.; Baldridge, K. K.; Boatz, J. A.; Elbert, S. T.; Gordon, M. S.; Jensen, J. H.; Koseki, S.; Matsunaga, N.; Nguyen, K. A.; Su, S. J.; et al. *Gamess*, version 11; Iowa State University: Ames, IA, 2008.
(35) Noury, S.; Krokidis, X.; Fuster, F.; Silvi, B. *ToPMoD*; Université Pierre et Marie Curie: Paris, France, 1999.
(36) Silvi, B.; Savin, A. *Nature* **1994**, *371*, 683−686.
(37) Ditchfield, R. *Mol. Phys.* **1974**, *27*, 789−807.
(38) Perera, S. A.; Nooijen, M.; Bartlett, R. J. *J. Chem. Phys.* **1996**, *104*, 3290−3305.
(39) Perera, S. A.; Sekino, H.; Bartlett, R. J. *J. Chem. Phys.* **1994**, *101*, 2186−2196.
(40) Schäfer, A.; Horn, H.; Ahlrichs, R. *J. Chem. Phys.* **1992**, *97*, 2571−2577.
(41) Stanton, J. F.; Gauss, J.; Watts, J. D.; Nooijen, M.; Oliphant, N.; Perera, S. A.; Szalay, P. S.; Lauderdale, W. J.; Gwaltney, S. R.; et al. *ACES II*; University of Florida: Gainesville, FL.
(42) Alkorta, I.; Elguero, J. *Struct. Chem.* **2004**, *15*, 117−120.
(43) Tang, T. H.; Deretey, E.; Knak Jensen, S. J.; Csizmadia, I. G. *Eur. Phys. J. D* **2006**, *37*, 217−222.
(44) Vener, M. V.; Manaev, A. V.; Egorova, A. N.; Tsirelson, V. G. *J. Phys. Chem. A* **2007**, *111*, 1155−1162.
(45) Mata, I.; Alkorta, I.; Molins, E.; Espinosa, E. *Chem.—Eur. J.* **2010**, *16*, 2442−2452.
(46) Zeng, Y.; Li, X.; Zhang, X.; Zheng, S.; Meng, L. *J. Mol. Model.* **2011**, *17*, 2907−2918.
(47) Zhang, X.; Zeng, Y.; Li, X.; Meng, L.; Zheng, S. *Struct. Chem.* **2011**, *22*, 567−576.
(48) Sánchez-Sanz, G.; Trujillo, C.; Alkorta, I.; Elguero, J. *ChemPhysChem* **2012**, *23*, 847−856.
(49) Espinosa, E.; Alkorta, I.; Elguero, J.; Molins, E. *J. Chem. Phys.* **2002**, *117*, 5529−5542.
(50) Rozas, I.; Alkorta, I.; Elguero, J. *J. Am. Chem. Soc.* **2000**, *122*, 11154−11161.
(51) Ziółkowski, M.; Grabowski, S. J.; Leszczynski, J. *J. Phys. Chem. A* **2006**, *110*, 6514−6521.